

pubs.acs.org/JACS Communication

Molecular Basis of CLC Antiporter Inhibition by Fluoride

Maria Gabriella Chiariello,* Viacheslav Bolnykh, Emiliano Ippoliti, Simone Meloni, Jógvan Magnus Haugaard Olsen, Thomas Beck, Ursula Rothlisberger, Christoph Fahlke,* and Paolo Carloni*

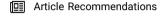


Cite This: https://dx.doi.org/10.1021/jacs.9b13588



ACCESS

Metrics & More



Supporting Information

ABSTRACT: CLC channels and transporters conduct or transport various kinds of anions, with the exception of fluoride, which acts as an effective inhibitor. Here, we performed sub-nanosecond DFT-based QM/MM simulations of the *E. coli* anion/proton exchanger ClC-ec1 and observed that fluoride binds incoming protons within the selectivity filter, with excess protons shared with the gating glutamate E148. Depending on E148 conformation, the competition for the proton can involve either a direct F⁻/E148 interaction or the modulation of water molecules bridging the two anions. The direct interaction locks E148 in a conformation that does not allow for proton transport, and thus inhibits protein function.

The CLC family encompasses anion channels and anion/proton exchangers across the three kingdoms of life¹⁻⁶ and fulfills various cell functions. Human CLC channels and transporters contribute to the regulation of cellular excitability, epithelial ion transport, or Cl⁻ and pH homeostasis in intracellular organelles.⁷⁻⁹ Mutations in genes encoding these proteins cause a variety of diseases, including muscle overexcitability, deafness, epilepsy, intellectual disability, nephrolithiasis, and osteopetrosis.^{10,11} The significant physiological importance as well as the intriguing coexistence of voltage-gated anion channels and anion/proton transporters in one gene family makes the CLC family a highly interesting topic for studying the chemical basis of transmembrane ion transport.

The Cl⁻/H⁺ antiporter ClC-ec1 was the first member of the CLC family that was studied by X-ray crystallography. 12,13 The protein mediates the transmembrane exchange of Cl⁻ for H⁺ with a 2:1 stoichiometry. 14 Anion/proton exchange occurs in a permeation pathway limited by two glutamates, one pointing toward the intracellular side (E203, the so-called proton glutamate)12,15 and the other toward the extracellular side (E148, the so-called gating glutamate). 12,14,16,17 Protons from the cytosol bind the carboxyl group of E203 and subsequently reach E148 via a water wire 18-21 between these two residues. After protonation, E148 rotates outward and thus exposes itself to the external side of the channel (from a down to an up conformation), to release the proton to the extracellular side and to open a permeation pathway that allows for chloride transit. 12,22,23 CLC anion channels and transporters allow for the transport of various anions, with significant permeability not only for Cl⁻ but also for larger and polyatomic anions, such as Br⁻, I⁻, NO₃⁻, and SCN⁻.²⁴⁻²⁸

Transport of F⁻ anion, which is smaller than Cl⁻,²⁹ has not been extensively studied across the CLC proteins. Intriguingly, it is negligibly permeant through CLC-1 and CLC-2,^{25,30} and it inhibits anion/proton exchange in ClC-ecl.^{25,31-33}

Indeed, flux assays and current measurements show that reconstituted transporters do not transport F^- . Fluoride efflux from CLC-ec1-containing liposomes is indistinguishable from protein-free liposomes,³³ while other anions can pass the protein-containing liposomes even without exchange with H^+ .²⁷ Neutralization of the gating glutamate by mutation to Ala permits high F^- conductance and effective F^- equilibrium binding.³³ In contrast, mutants that only disrupt the anion pathway's inner gate (Y445A) or impair H^+ binding from the cytoplasmic side (E203Q) are still highly selective for Cl^- over F^- .^{33,34} Hence, F^- inhibition is likely to be caused by specific F^- — H^+ interactions at the central binding site, rather than by a strong Cl^- / F^- selectivity of the anion conduction pathway.

X-ray studies on E148Q ClC-ec1 show that Q148 (in *down* conformation) directly interacts with the F⁻ within a hydrogen bond distance.³³ A neutral E148 in *down* conformation could keep F⁻ blocked in the protein binding site through a strong hydrogen bond interaction, whereas protonation of E148 triggers the *down/up* transition and hence proton release to the extracellular side with chloride as the main anion and in the absence of fluoride.^{18,22}

Here, we investigate the molecular basis of fluoride inhibition on the ClC-ec1 transport cycle by multiscale molecular simulations. Our model system consists of the CLC-ec1 X-ray structure, 12 embedded in a POPC 35,36 bilayer in the presence of counterions (Figure 1), in which F⁻ replaces the Cl⁻ in the central binding site in both the subunits. Our project takes advantage of a recently developed, massively parallel DFT-based QM/MM interface between the CPMD

Received: December 17, 2019 Published: April 1, 2020



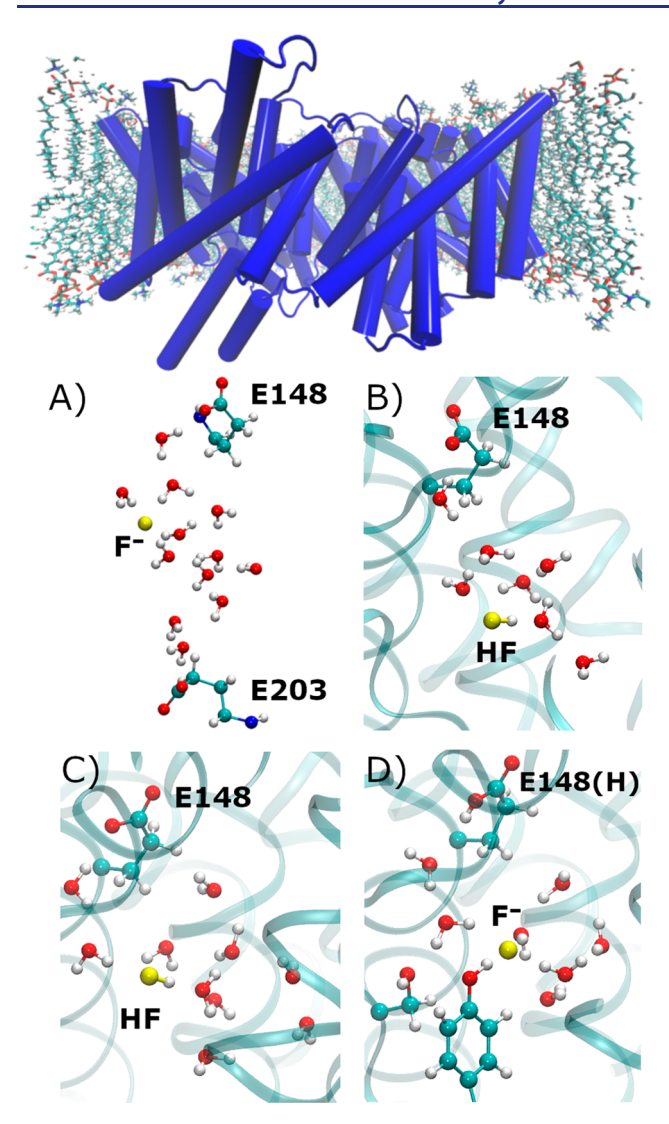


Figure 1. QM/MM MD simulations at the B3LYP/CHARMM level of theory for different initial proton locations. (Top panel) E. coli CLC antiporter (CLC-ec1) in a lipid bilayer. Water and counterions are not shown for clarity. (Bottom panel A) Snapshot from our classical MD simulation. Here 12 water molecules form a hydrogen bond network connecting E203, E148, and F (yellow sphere). The excess proton is added to different water molecules in five simulations. Only three are shown here. (B-D) QM/MM configurations after 0.5 ps. The proton, after hopping through a chain of water molecules, has already formed either H-F (B, C) or protonated E148 species (D). The starting configurations, as well as the other two trajectories, are depicted in Figure S3A-E. The QM region includes F⁻, E148, R147, hydronium, the water molecules connecting them, and (in D) also Y445 and S107.

and GROMACS codes^{37,38} that was run on the computational facilities at the Juelich Supercomputing Center. Overall, this has allowed us to model 16 ps of DFT-based QM/MM molecular dynamics (MD) and 455 ps of well-tempered metadynamics (MTD³⁹) free energy calculations^{37,38} (at the B3LYP^{40,41} and BLYP levels of theory, respectively). Since the crystallographic structure lacks water molecules inside the channel, we obtained the average solvation around the anion within the transporter core through 300 ns of classical MD simulations using the CHARMM force field.⁴²

The central region is hydrated with up to 12 water molecules, forming a continuous water chain connecting

E203 and E148 (Figures 1A and S1). The E148 side chain (in its deprotonated state) does not change conformation during the simulation time (Figure S2).

On average, two water molecules lie in between E148 and F and four solvent molecules coordinate the fluoride in its binding site, where Y445 and S107 side chains complete the coordination around the anion with either direct or watermediated H-bonds (Figures S1 and S2).

As mentioned above, the proton transfer (PT) from E203 to E148 is a crucial step in ClC-ec1 proton transport. 19,22

We performed five independent QM/MM MD simulations, in which one proton is added in different positions of the water network connecting F⁻, E203, and E148 (Figure 1A). In all circumstances, PT processes via the water wire occur already within less than 1 ps, either to E148 or to F-, leading to the formation of HF. The resulting acids (protonated E148 and HF) do not dissociate afterward (Figure S3A-E). No significant conformational changes of E148 occurred over the remaining simulation time. The formation of a stable HF molecule is fully consistent with the well-known halogens' acid-base properties: HF dissociation in water is rather unfavorable ($\Delta G = 4.3 \text{ kcal/mol}$), while this is not the case for other binary acids including HCl ($\Delta G = -9.5 \text{ kcal/mol}^{29}$). However, in the case of the Cl⁻ ion, the PT process toward the E148 could include a transient state in which the proton binds the chloride for a short time, 43 while a direct interference of the F- with the excess proton has only been hypothesized so far.44

Next, we investigate whether E203 may affect these PT pathways. By including E203 and its hydration sphere in the QM region, our QM/MM simulations mostly reproduced the same results as above. Yet, in one QM/MM simulation, the proton does migrate to E203 (Figure S4E). We thus conclude that, in the presence of fluoride, E203 only serves as part of the proton pathways toward the two negatively charged groups, while playing no role for fluoride inhibition as proton acceptor, as established by the experiments.³³

To estimate the relative stability of the two states characterized by the proton bound to either the F⁻ anion or E148, we investigated the free energy landscape associated with the PT between the two anions with two intervening water molecules (Figure 2A) via QM/MM MTD simulations. The free energy, as a function of chosen collective variables (the fluoride- and E148-proton distances), shows two minima at d(H-F) = 1.0 Å, d(H-E148) = 1.7 Å and d(H-E148) = 1.7 ÅF) = 1.6 Å, d(H-E148) = 1.0 Å, corresponding to the two protonation states (Figure 2A). The minima are similar in free energy (~1 kcal/mol), and they are separated by a free energy barrier of a few kcal/mol⁴⁵ (Figure S5). In this conformation, the proton goes back and forth, through two water molecules, from F⁻ to E148 in a kind of competition/sharing mechanism. The position of the E148 side chain may change depending on its protonation state. 18,22 In particular, the calculations so far relied on the E148 crystallographic conformation, in which the carboxylic side chain is exposed to the external side of the permeation pathway (up). In contrast, E148 in its down conformation is exposed to the inner part of the channel, where it can interact with the anion. We therefore investigated the down/up conformational change by calculating the associated free energy as a function of E148's N-C α -C β - $C\gamma$ (χ_1) torsional angle, which dictates the transition (Figure 2C and D). In both cases the anion is present in the binding

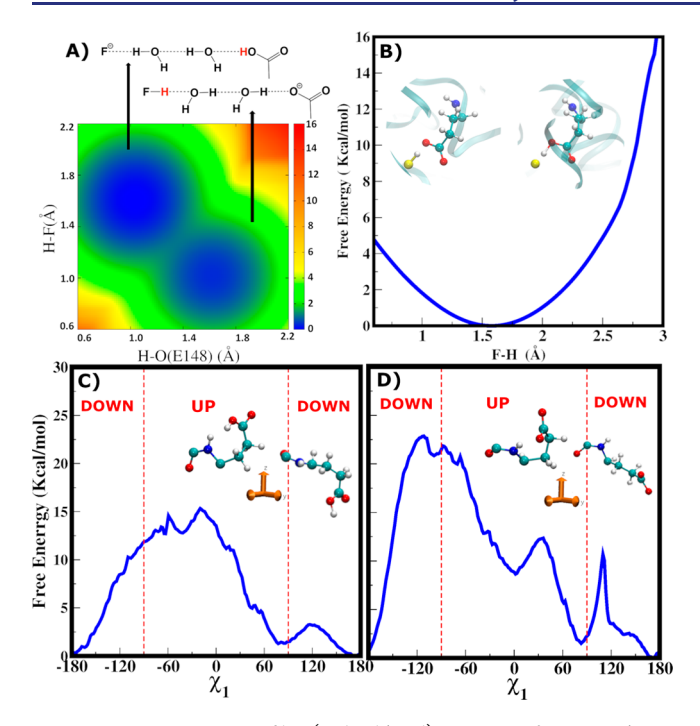


Figure 2. Free energy profiles (in kcal/mol) emerging from QM/MM MTD simulations at the BLYP/CHARMM level of theory. (A) Free energy associated with the PT process between fluoride and E148 modulated by two water molecules. The schematic representation of the two free energy minima is displayed on the top of the figure. Here, E148 is in the *up* conformation. (B) Free energy profile associated with the direct PT process between F⁻ and E148 in the *down* conformation. The minimum is reached at H–F and H–O(E148) (Figure S8D) distances of 1.5 and 1.0 Å, respectively. No barrier separates the state in which the proton is bound to the fluoride (H–F 1.0 Å). (C, D) Free energy as a function of E148's χ_1 dihedral angle for E148 protonated (C) and deprotonated (D). The relative positions of the E148 carboxyl group above or below the backbone unit define the *up or down* conformations. The transition from one conformation to the other is indicated by dashed red lines.

site as F⁻ and HF when E148 is protonated and deprotonated, respectively.

In the presence of F⁻ anion, the *down* conformation is far more favored than the *up* one regardless of the protonation state, in agreement with previous calculations. ^{23,46} In addition, *up* is a local minimum only if E148 is deprotonated (Figure 2C and D). Upon protonation, the $up \rightarrow down$ transition is actually a barrierless process. There is no longer a minimum near the *up* conformation region.

Once exposed to the internal side of the channel, E148 can form a direct hydrogen bond with F^- . To investigate the nature of this interaction, we performed an MTD-based free energy calculation using the H–F distance as a collective variable. It turns out that the proton is fully shared by fluoride and E148, as shown by the presence of a single minimum in the H–F free energy (Figure 2B). This may be consistent with the similarities of the pK_a value of Glu $(4.2)^{47}$ and HF $(3.2)^{.29}$ While this direct interaction was invoked already as the key structural determinant for the inhibition mechanism, ³³ our findings point to a much more complex scenario than a simple H-bond interaction: the H–F distance ranges between 1 Å (HF–E148) and 2 Å (F–HE148, Figure 2B).

Bringing the proton from its complex with E148 and F⁻ to the bulk requires the $down \rightarrow up$ transition of the protonated

E148. The estimated free energy barrier of this transition (\sim 15 kcal/mol, Figure 2C) is much higher than the corresponding one for chloride (5 kcal/mol). The inverse ($up \rightarrow down$) process is basically barrierless (Figure 2C), leading to the rather stable F-H-E148 triad structure (Figure 2B).

These considerations lead us to suggest the following mechanism of inhibitions: protons coming from the extracellular side will migrate spontaneously to the protein cavity and will be trapped there by E148 (in a *down* conformation) and F^- (Figure 2B). This explanation is consistent with the available experimental data on CLC-ec1, from the formation of a fluoride-Gln H-bond in the E148Q mutant to the fact that the E148A variant allows for F^- transport.³³

In conclusion, we here identify the high affinity of both F⁻ and E148 for protons as the basis of the transport inhibition of the CLC anion/proton exchangers from *E. coli*. Our hypothesis predicts impaired fluoride inhibition of CLC channels that lack a glutamate at this position, like the renal CLC-K, ⁴⁹ and restored block in mutant channels with reinserted glutamate. ⁵⁰ The comparative analysis of fluoride inhibition in multiple CLC channels and transporters, some of which differ in binding affinity and selectivity of binding sites within the anion transport pathway, ⁵¹ may identify additional determinants of fluoride block across this important anion channel/transporter family.

ASSOCIATED CONTENT

Supporting Information

The Supporting Information is available free of charge at https://pubs.acs.org/doi/10.1021/jacs.9b13588.

Computational details for the system setup, classical MD, QM/MM, and QM/MM MTD simulations; hydration and structural analysis of the MD simulations; snapshots of the QM/MM dynamics illustrating the proton pathways; convergence of the FE profiles; population analysis (PDF)

AUTHOR INFORMATION

Corresponding Authors

Maria Gabriella Chiariello — Institute for Advanced Simulation (IAS-5) and Institute of Neuroscience and Medicine (INM-9), Computational Biomedicine and JARA-HPC, Forschungszentrum Jülich, 52425 Jülich, Germany; orcid.org/0000-0003-1076-682X; Email: g.chiariello@fziuelich.de

Christoph Fahlke — Institute of Biological Information Processing (IBI-1), Molekular- und Zellphysiologie, Forschungszentrum Jülich, D-54245 Jülich, Germany; Email: c.fahlke@fz-juelich.de

Paolo Carloni — Institute for Advanced Simulation (IAS-5) and Institute of Neuroscience and Medicine (INM-9), Computational Biomedicine and JARA-HPC, Forschungszentrum Jülich, 52425 Jülich, Germany; Department of Physics, RWTH Aachen University, 52056 Aachen, Germany; Institute of Neuroscience and Medicine (INM-11), Molecular Neuroscience and Neuroimaging, Forschungszentrum Julich, 52425 Julich, Germany; orcid.org/0000-0002-9010-0149; Email: p.carloni@fz-juelich.de

Authors

- Viacheslav Bolnykh Laboratory of Computational Chemistry and Biochemistry, Ecole Polytechnique Federale de Lausanne, CH-1015 Lausanne, Switzerland
- Emiliano Ippoliti Institute for Advanced Simulation (IAS-5) and Institute of Neuroscience and Medicine (INM-9), Computational Biomedicine and JARA-HPC, Forschungszentrum Jülich, 52425 Jülich, Germany; orcid.org/0000-0001-5513-8056
- Simone Meloni Dipartimento di Scienze Chimiche e Farmaceutiche, Università degli Studi di Ferrara, I-44121 Ferrara, Italy
- Jógvan Magnus Haugaard Olsen Hylleraas Centre for Quantum Molecular Sciences, Department of Chemistry, UiT The Arctic University of Norway, N-9037 Tromsø, Norway; orcid.org/0000-0001-7487-944X
- Thomas Beck Department of Chemistry, University of Cincinnati, Cincinnati, Ohio 4S221, United States
- Ursula Rothlisberger Laboratory of Computational Chemistry and Biochemistry, Ecole Polytechnique Federale de Lausanne, CH-1015 Lausanne, Switzerland; orcid.org/ 0000-0002-1704-8591

Complete contact information is available at: https://pubs.acs.org/10.1021/jacs.9b13588

Notes

The authors declare no competing financial interest.

ACKNOWLEDGMENTS

The authors gratefully acknowledge the computing time granted through JARA-HPC on the supercomputer JURECA⁵² at Forschungszentrum Jülich (Project ID: jias5f). J.M.H.O. acknowledges financial support from the Research Council of Norway through its Centers of Excellence scheme (Project ID: 262695). T.L.B. acknowledges the support of the U.S. National Science Foundation grants CHE-15656632 and CHE-1955161 for partial support of this research. M.G.C., C.F., and P.C. acknowledge the funding by the Deutsche Forschungsgemeinschaft via FOR 2518 DynIon project P6. P.C. thanks the support of BioExcel (www.bioexel.eu), a project funded by the European Union contracts H2020-INFRAEDI-02-2018-823830 and H2020-EINFRA-2015-1-675728.

REFERENCES

- (1) Jentsch, T. J.; Pusch, M. CLC Chloride Channels and Transporters: Structure, Function, Physiology, and Disease. *Physiol. Rev.* **2018**, *98* (3), 1493–1590.
- (2) Picollo, A.; Pusch, M. Chloride/proton antiporter activity of mammalian CLC proteins ClC-4 and ClC-5. *Nature* **2005**, 436 (7049), 420–423.
- (3) Jentsch, T. J. CLC Chloride Channels and Transporters: From Genes to Protein Structure, Pathology and Physiology. *Crit. Rev. Biochem. Mol. Biol.* **2008**, 43 (1), 3–36.
- (4) Accardi, A. Structure and gating of CLC channels and exchangers. J. Physiol. 2015, 593 (18), 4129-4138.
- (5) Feng, L.; Campbell, E. B.; Hsiung, Y.; MacKinnon, R. Structure of a Eukaryotic CLC Transporter Defines an Intermediate State in the Transport Cycle. *Science* **2010**, *330* (6004), 635.
- (6) Park, E.; Campbell, E. B.; MacKinnon, R. Structure of a CLC chloride ion channel by cryo-electron microscopy. *Nature* **2017**, *S41* (7638), 500–505.
- (7) Stölting, G.; Fischer, M.; Fahlke, C. CLC channel function and dysfunction in health and disease. *Front. Physiol.* **2014**, *5*, 378.

- (8) Poroca, D. R.; Pelis, R. M.; Chappe, V. M. ClC Channels and Transporters: Structure, Physiological Functions, and Implications in Human Chloride Channelopathies. *Front. Pharmacol.* **2017**, *8*, 151.
- (9) Jentsch, T. J.; Stein, V.; Weinreich, F.; Zdebik, A. A. Molecular Structure and Physiological Function of Chloride Channels. *Physiol. Rev.* **2002**, *82* (2), 503–568.
- (10) Stauber, T.; Weinert, S.; Jentsch, T. J. Cell Biology and Physiology of CLC Chloride Channels and Transporters. *Compr. Physiol.* **2012**, 1701–1744.
- (11) Jentsch, T. J. Discovery of CLC transport proteins: cloning, structure, function and pathophysiology. *J. Physiol.* **2015**, *5*93 (18), 4091–4109.
- (12) Dutzler, R.; Campbell, E. B.; MacKinnon, R. Gating the Selectivity Filter in ClC Chloride Channels. *Science* **2003**, *300* (5616), 108
- (13) Dutzler, R.; Campbell, E. B.; Cadene, M.; Chait, B. T.; MacKinnon, R. X-ray structure of a ClC chloride channel at 3.0 Å reveals the molecular basis of anion selectivity. *Nature* **2002**, *415* (6869), 287–294.
- (14) Accardi, A.; Miller, C. Secondary active transport mediated by a prokaryotic homologue of ClC Cl- channels. *Nature* **2004**, 427 (6977), 803–807.
- (15) Accardi, A.; Walden, M.; Nguitragool, W.; Jayaram, H.; Williams, C.; Miller, C. Separate Ion Pathways in a Cl⁻/H⁺ Exchanger. *J. Gen. Physiol.* **2005**, *126* (6), 563.
- (16) Picollo, A.; Xu, Y.; Johner, N.; Bernèche, S.; Accardi, A. Synergistic substrate binding determines the stoichiometry of transport of a prokaryotic H⁺/Cl⁻ exchanger. *Nat. Struct. Mol. Biol.* **2012**, *19* (5), 525–531.
- (17) Lim, H.-H.; Miller, C. Intracellular Proton-Transfer Mutants in a CLC Cl⁻/H⁺ Exchanger. *J. Gen. Physiol.* **2009**, 133 (2), 131.
- (18) Lee, S.; Swanson, J. M. J.; Voth, G. A. Multiscale Simulations Reveal Key Aspects of the Proton Transport Mechanism in the ClC-ec1 Antiporter. *Biophys. J.* **2016**, *110* (6), 1334–1345.
- (19) Jiang, T.; Han, W.; Maduke, M.; Tajkhorshid, E. Molecular Basis for Differential Anion Binding and Proton Coupling in the Cl⁻/H⁺ Exchanger ClC-ec1. *J. Am. Chem. Soc.* **2016**, *138* (9), 3066–3075.
- (20) Wang, Z.; Swanson, J. M. J.; Voth, G. A. Modulating the Chemical Transport Properties of a Transmembrane Antiporter via Alternative Anion Flux. J. Am. Chem. Soc. 2018, 140 (48), 16535–16543.
- (21) Wang, Z.; Swanson, J. M. J.; Voth, G. A. Local conformational dynamics regulating transport properties of a Cl⁻/H⁺ antiporter. *J. Comput. Chem.* **2020**, *41* (6), 513–519.
- (22) Lee, S.; Mayes, H. B.; Swanson, J. M. J.; Voth, G. A. The Origin of Coupled Chloride and Proton Transport in a Cl^-/H^+ Antiporter. *J. Am. Chem. Soc.* **2016**, *138* (45), 14923–14930.
- (23) Mayes, H. B.; Lee, S.; White, A. D.; Voth, G. A.; Swanson, J. M. J. Multiscale Kinetic Modeling Reveals an Ensemble of Cl^-/H^+ Exchange Pathways in ClC-ec1 Antiporter. *J. Am. Chem. Soc.* **2018**, 140 (5), 1793–1804.
- (24) Fahlke, C.; Dürr, C.; George, A. L. Mechanism of Ion Permeation in Skeletal Muscle Chloride Channels. *J. Gen. Physiol.* 1997, 110 (5), 551.
- (25) Rychkov, G. Y.; Pusch, M.; Roberts, M. L.; Jentsch, T. J.; Bretag, A. H. Permeation and Block of the Skeletal Muscle Chloride Channel, ClC-1, by Foreign Anions. *J. Gen. Physiol.* **1998**, *111* (5), 653.
- (26) Alekov, A. K.; Fahlke, C. Channel-like slippage modes in the human anion/proton exchanger ClC-4. *J. Gen. Physiol.* **2009**, *133* (5), 485.
- (27) Nguitragool, W.; Miller, C. Uncoupling of a CLC Cl^-/H^+ Exchange Transporter by Polyatomic Anions. *J. Mol. Biol.* **2006**, 362 (4), 682–690.
- (28) Fahlke, C.; Beck, C. L.; George, A. L. A mutation in autosomal dominant myotonia congenita affects pore properties of the muscle chloride channel. *Proc. Natl. Acad. Sci. U. S. A.* 1997, 94 (6), 2729.

- (29) Cotton, F. A.; Wilkinson, G.; Murillo, C. A.; Bochmann, M.; Grimes, R. *Advanced Inorganic Chemistry*; Wiley: New York, 1988; Vol. 6.
- (30) De Jesús-Pérez, J. J.; Castro-Chong, A.; Shieh, R.-C.; Hernández-Carballo, C. Y.; De Santiago-Castillo, J. A.; Arreola, J. Gating the glutamate gate of CLC-2 chloride channel by pore occupancy. *J. Gen. Physiol.* **2016**, *147* (1), 25–37.
- (31) Maduke, M.; Pheasant, D. J.; Miller, C. High-Level Expression, Functional Reconstitution, and Quaternary Structure of a Prokaryotic Clc-Type Chloride Channel. J. Gen. Physiol. 1999, 114 (5), 713.
- (32) Fahlke, C. Ion permeation and selectivity in ClC-type chloride channels. Am. J. Physiol. Renal. Physiol. 2001, 280 (5), F748-F757.
- (33) Lim, H.-H.; Stockbridge, R. B.; Miller, C. Fluoride-dependent interruption of the transport cycle of a CLC Cl⁻/H⁺ antiporter. *Nat. Chem. Biol.* **2013**, *9*, 721.
- (34) These studies further indicate that there is no leak of proton permeability in the presence of F—.
- (35) Gervasio, F. L.; Parrinello, M.; Ceccarelli, M.; Klein, M. L. Exploring the Gating Mechanism in the ClC Chloride Channel via Metadynamics. *J. Mol. Biol.* **2006**, *361* (2), 390–398.
- (36) Leisle, L.; Xu, Y.; Fortea, E.; Galpin, J.; Vien, M.; Ahern, C. A.; Accardi, A.; Bernèche, S. Divergent Cl⁻ and H⁺ pathways underlie transport coupling and gating in CLC exchangers and channels. bioRxiv 2019, 753954.
- (37) Olsen, J. M. H.; Bolnykh, V.; Meloni, S.; Ippoliti, E.; Bircher, M. P.; Carloni, P.; Rothlisberger, U. MiMiC: A Novel Framework for Multiscale Modeling in Computational Chemistry. *J. Chem. Theory Comput.* **2019**, *15* (6), 3810–3823.
- (38) Bolnykh, V.; Olsen, J. M. H.; Meloni, S.; Bircher, M. P.; Ippoliti, E.; Carloni, P.; Rothlisberger, U. Extreme Scalability of DFT-Based QM/MM MD Simulations Using MiMiC. *J. Chem. Theory Comput.* **2019**, *15* (10), 5601–5613.
- (39) Barducci, A.; Bonomi, M.; Parrinello, M. Metadynamics. Wiley Interdiscip. Rev.: Comput. Mol. Sci. 2011, 1 (5), 826–843.
- (40) Becke, A. D. Density-functional thermochemistry. I. The effect of the exchange-only gradient correction. *J. Chem. Phys.* **1992**, *96* (3), 2155–2160.
- (41) Becke, A. D. Density-functional thermochemistry. II. The effect of the Perdew–Wang generalized-gradient correlation correction. *J. Chem. Phys.* **1992**, *97* (12), 9173–9177.
- (42) Mackerell, A. D., Jr; Feig, M.; Brooks Iii, C. L. Extending the treatment of backbone energetics in protein force fields: Limitations of gas-phase quantum mechanics in reproducing protein conformational distributions in molecular dynamics simulations. *J. Comput. Chem.* **2004**, 25 (11), 1400–1415.
- (43) Duster, A. W.; Garza, C. M.; Aydintug, B. O.; Negussie, M. B.; Lin, H. Adaptive Partitioning QM/MM for Molecular Dynamics Simulations: 6. Proton Transport through a Biological Channel. *J. Chem. Theory Comput.* **2019**, *15* (2), 892–905.
- (44) Chen, Z.; Beck, T. L. Free Energies of Ion Binding in the Bacterial CLC-ec1 Chloride Transporter with Implications for the Transport Mechanism and Selectivity. *J. Phys. Chem. B* **2016**, *120* (12), 3129–3139.
- (45) Here the BLYP exchange—correlation functional, much less computationally demanding than B3LYP, is used in combination with MTD to ensure the convergence of the free energy landscape. BLYP can predict qualitatively trends in energy differences (Hassanali, A.; Giberti, F.; Cuny, J.; Kühne, T. D.; Parrinello, M., Proton transfer through the water gossamer. *Proc. Natl. Acad. Sci.* 2013, 110 (34), 13723). Hence we expect the two minima to exhibit not too dissimilar free energies also when using higher level calculations. This contrasts with the free energy barriers (here calculated as ~1.8 kcal/mol), expected to be underestimated by the BLYP functional.
- (46) Kuang, Z.; Mahankali, U.; Beck, T. L. Proton pathways and H⁺/Cl⁻ stoichiometry in bacterial chloride transporters. *Proteins: Struct., Funct., Genet.* **2007**, *68* (1), 26–33.
- (47) Grimsley, G. R.; Scholtz, J. M.; Pace, C. N. A summary of the measured pK values of the ionizable groups in folded proteins. *Protein Sci.* **2008**, *18* (1), 247–251.

- (48) We estimate that at least 5 kcal/mol is required to disrupt the complex (see Section 5 in the SI for details).
- (49) Uchida, S.; Sasaki, S. Function of chloride channels in the kidney *Annu. Annu. Rev. Physiol.* **2005**, *67* (1), 759–778.
- (50) Scholl, U.; Hebeisen, S.; Janssen, A. G. H.; Müller-Newen, G.; Alekov, A.; Fahlke, C. Barttin modulates trafficking and function of CIC-K channels. *Proc. Natl. Acad. Sci. U. S. A.* **2006**, *103* (30), 11411.
- (51) De Angeli, A.; Monachello, D.; Ephritikhine, G.; Frachisse, J. M.; Thomine, S.; Gambale, F.; Barbier-Brygoo, H. The nitrate/proton antiporter AtCLCa mediates nitrate accumulation in plant vacuoles. *Nature* **2006**, 442 (7105), 939–942.
- (52) Jülich Supercomputing Centre. (2018) JURECA: Modular supercomputer at Juelich Supercomputing Centre. *J. Large-Scale Res. Fac.*, 4, http://dx.doi.org/10.17815/jlsrf-4-121-1.